Journal of Alloys and Compounds 509 (2011) 4426–4432

Contents lists available at ScienceDirect

Journal of Alloys and Compounds

journal homepage: www.elsevier.com/locate/jallcom

Effects of protecting layer [Li,La]TiO_3 on electrochemical properties of $LiMn_2O_4$ for lithium batteries

Kwang Hee Jung[a], Ho-Gi Kim[a], Yong Joon Park[b,*]

[a] Department of Materials Science and Engineering, Korea Advanced Institute of Science and Technology, Daejeon 305-701, Republic of Korea
[b] Department of Advanced Materials Engineering, Kyonggi University, Gyeonggi-do 443-760, Republic of Korea

ARTICLE INFO

Article history:
Received 9 November 2010
Received in revised form 18 January 2011
Accepted 18 January 2011
Available online 25 January 2011

Keywords:
Energy storage materials
Electrochemical reactions
$LiMn_2O_4$
[Li,La]TiO_3
Cathode material
Surface modification

ABSTRACT

A sample of $LiMn_2O_4$ spinel oxide was surface-modified with lithium lanthanum titanate ([Li,La]TiO_3), which was developed as a lithium ionic conductor, by means of hydrothermal processing and subsequent heat treatment at 400 °C. The surface coating layers were analyzed by morphology observation using a transmission electron microscopy. Energy-dispersive spectrometry and X-ray photoelectron spectroscopy were used for element investigation. The surface modification effects on rate capability during cycling and capacity retention for the $LiMn_2O_4$ spinel oxide were confirmed. Then Mn dissolution during storage at elevated temperatures of the pristine, coated sample was characterized. The Mn dissolution characterization was based on the idea that Mn dissolution is one of the most significant reasons for capacity loss for $LiMn_2O_4$ spinel oxide, and this phenomenon is especially severe at elevated temperatures. Our experimental results indicate that the surface-modified sample shows much a better initial capacity and rate capability compared with the pristine sample. The [Li,La]TiO_3 coating effectively enhances the structural stability of $LiMn_2O_4$ at elevated temperatures, most likely because the [Li,La]TiO_3-modifying layers play a definitive role in suppressing Mn dissolution in the electrolyte during storage.

1. Introduction

The low cost and low toxicity of $LiMn_2O_4$ have created intense research interest in its use as a replacement of $LiCoO_2$ [1–7]. However, the large capacity loss of $LiMn_2O_4$ during the cycling phase discourages any commercial use of the material. The capacity fading during cycling is attributed to various factors, such as manganese dissolution in the electrolyte [8–10], Jahn–Teller distortion [11,12], and the formation of an oxygen deficiency [13]. To overcome these problems, many efforts have been devoted to modify the problems originating from the intrinsic characteristics of $LiMn_2O_4$. Cation doping is considered to be an effective strategy to improve the problems of $LiMn_2O_4$ by means of a series of transition metal-substituted spinel lithium manganese oxides [10,14–16]. However, Mn dissolution resulted from some side reactions that occurred at the interface between the electrode and the electrolyte during the charge/discharge process [2], and the interfacial reaction between the active material and the electrolyte plays a significant role in lithium secondary batteries [17]. In order to solve this problem, surface modification of the cathode material is an effective method to reduce the side reactions [2,9,10]. Researchers have focused on the surface modification of $LiMn_2O_4$ by means of ZrO_2 [9], CeO_2 [10], MgO [18], Al_2O_3 [19], and $LiNi_{1/2}Mn_{1/2}O_2$ [20]. The modification effects correlate highly with the modifying material. Therefore, the task of determining the appropriate modifying material for a modified cathode material is crucial.

In this study, [Li,La]TiO_3 was used as the surface-modifying material. This perovskite-type compound has received considerable attention as a solid electrolyte due to its high lithium ionic conductivity [21–27] in contrast to most existing researched surface-modifying materials that are basically nonconductive materials of lithium ions and electrons and may consequently act as an obstacle to the diffusion of lithium ions. Surface modification can enhance the properties of the cathode material because it can suppress the formation of any unwanted surface layer that may originate from the dissolution of cations or an attack of HF on the electrolyte [28–30]. However, it is possible that the surface coating layer itself is a hindrance to the diffusion of lithium ions and electrons. It is expected that a $LiMn_2O_4$ electrode coated with [Li,La]TiO_3 will have a greater rate capability owing to the coating with high ionic and electronic conductivity. Aqueous rechargeable lithium batteries also suggest that these batteries can overcome some issues resulting from the use of organic electrolytes containing the decomposition of $LiPF_6$, which leads to the production of HF and lowers ionic conductivity more that in the aqueous ones [31,32]. In addition, the [Li,La]TiO_3 coating effect on the suppres-

* Corresponding author. Tel.: +82 31 249 9769; fax: +82 31 249 9769.
E-mail address: yjpark2006@kyonggi.ac.kr (Y.J. Park).

0925-8388/$ – see front matter © 2011 Elsevier B.V. All rights reserved.
doi:10.1016/j.jallcom.2011.01.110

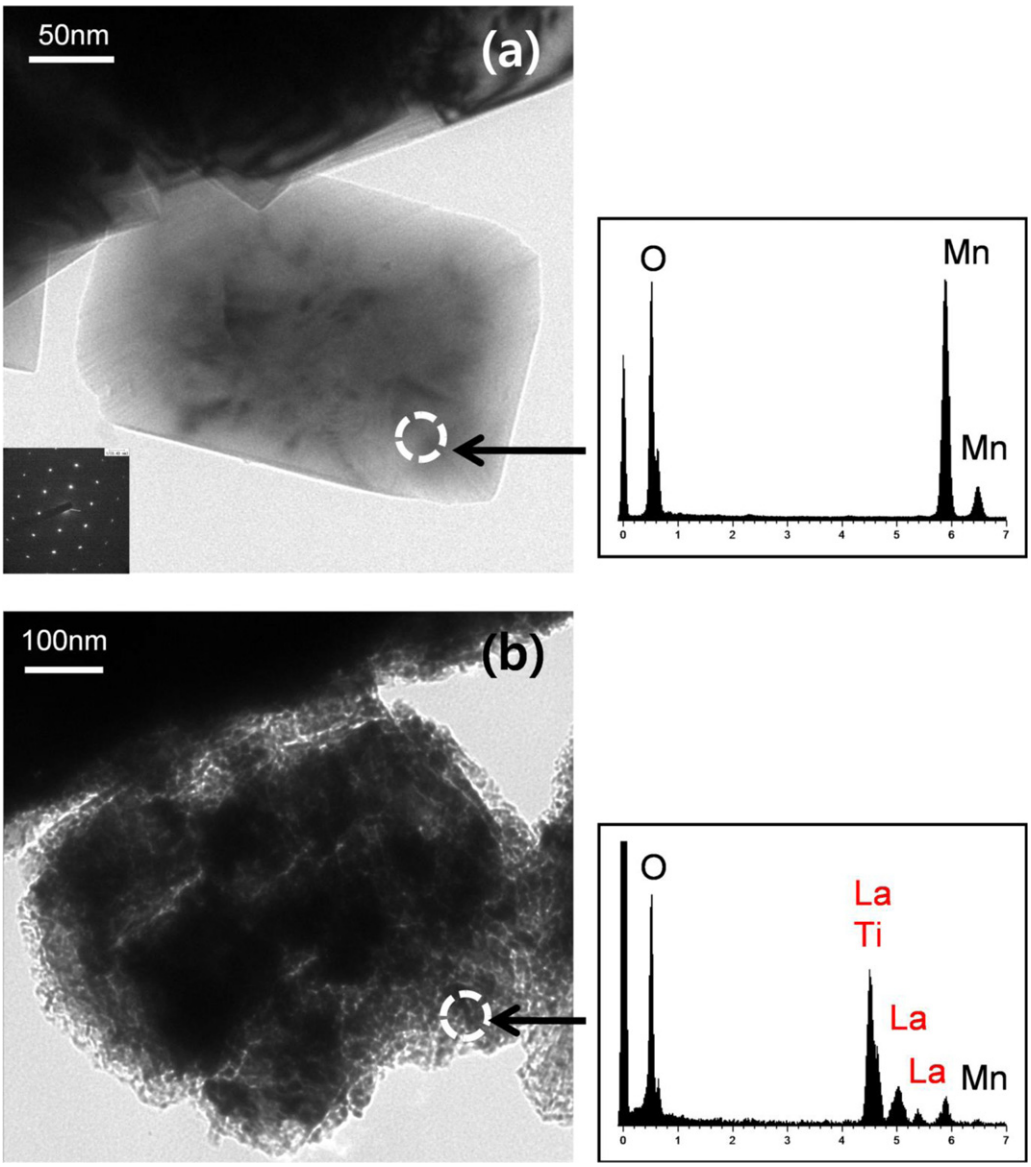

Fig. 1. TEM images and TEM-EDS peaks of the (a) pristine, (b) [Li,La]TiO_3-modified $LiMn_2O$.

sion of Mn dissolution of $LiMn_2O_4$ at the elevated temperature is the focus in this work.

Mn dissolution is one of the very significant factors in the deterioration of the electrochemical property of $LiMn_2O_4$ system during cycling. It is expected that a comparison between the pristine and surface modified $LiMn_2O_4$ after storage at elevated temperature is a useful research method because the Mn dissolution at elevated temperature is maximized.

2. Experimental

$LiMn_2O_4$ was prepared by a solid state synthesis from Li_2CO_3, MnO_2. The starting materials were mixed by ball milling; then the mixture was calcined at 600 °C for 5 h and 850 °C 10 h in air. To coat [Li,La]TiO_3 on the surface of the $LiMn_2O_4$ powder, $LiNO_3$, $La(NO_3)_3{\cdot}6H_2O$ and $Ti(OC_4H_9)O_4$ was dissolved in the ethanol. The amount of [Li,La]TiO_3 was 2 wt% of $LiMn_2O_4$ powders. Subsequently, NH_4OH solution was added to the solution to adjust the pH to 10. $LiMn_2O_4$ was then added to the solution and mixed thoroughly for 4 h at room temperature. The slurry containing $LiMn_2O_4$ powders was transferred to the Teflon-sealed stainless steel autoclave and sealed tightly. Thermal treatments were carried out at 80 °C for 10 h in autogenous pressure. The product was dried at 110 °C to remove residual water and then calcined at 400 °C for 5 h.

Cathodes were fabricated with the $LiMn_2O_4$ powders, Super-P carbon black, and polyvinylidene fluoride binder at a weight ratio of 80:12:8, respectively. CR2032 type coin cells were assembled using the prepared cathodes, lithium anodes, polypropylene separators, and electrolytes (1 M $LiPF_6$ dissolved in an equal-volume mixture of ethylene carbonate and dimethyl carbonate) in a glove box filled with Ar gas. Galvanostatic charge/discharge tests were carried out using a cycler in the voltage range of 3.0–4.3 V at room temperature and elevated temperature. For the electrochemical impedance spectroscopy (EIS), a frequency response analyzer (Solartron 1260 in conjunction with a Solartron 1287 electrochemical interface) was used. Impedance measurements were examined by applying an ac voltage of 10 mV over a frequency range of 0.1 Hz to 1 MHz.

X-ray diffraction patterns (XRD, RINT2000, Rigaku) were obtained using Cu Kα radiation. The microstructure of the particles was examined by a transmission electron microscope (TEM, JEM3010, 300 kV, JEOL). Information on the surface composition was examined by X-ray photoelectron spectroscopy (XPS, VG Scientific) and energy-dispersive spectrometry (EDS).

For the storage performance test, assembled CR2032 type coin cells were stored at 65 °C in an electrolyte solution and then the charge/discharge test of the batteries was carried out at 30 mA g^{-1} between 4.3 V and 3.0 V. This electrolyte solution (the powder stored at 65 °C for 200 h in this electrolyte solution) was used for inductively coupled plasma (PS1000UV Sequential ICP/Echelle) analysis. The morphology and depth profile of the electrodes after storage were obtained using TEM and glow discharge optical emission spectroscopy (GD-OES). For evaluating the electrodes after storage, the cathodes were washed with a DEC solution to remove the electrolyte salt. The samples for GD-OES analysis were sputtered in an argon atmosphere by applying radio frequency. The Radio Frequency Glow Discharge Spectrometer (JY 10000 RF, KBSI-PA314) at the Korea Basic Science Institute (Busan Center) was used for the measurement.

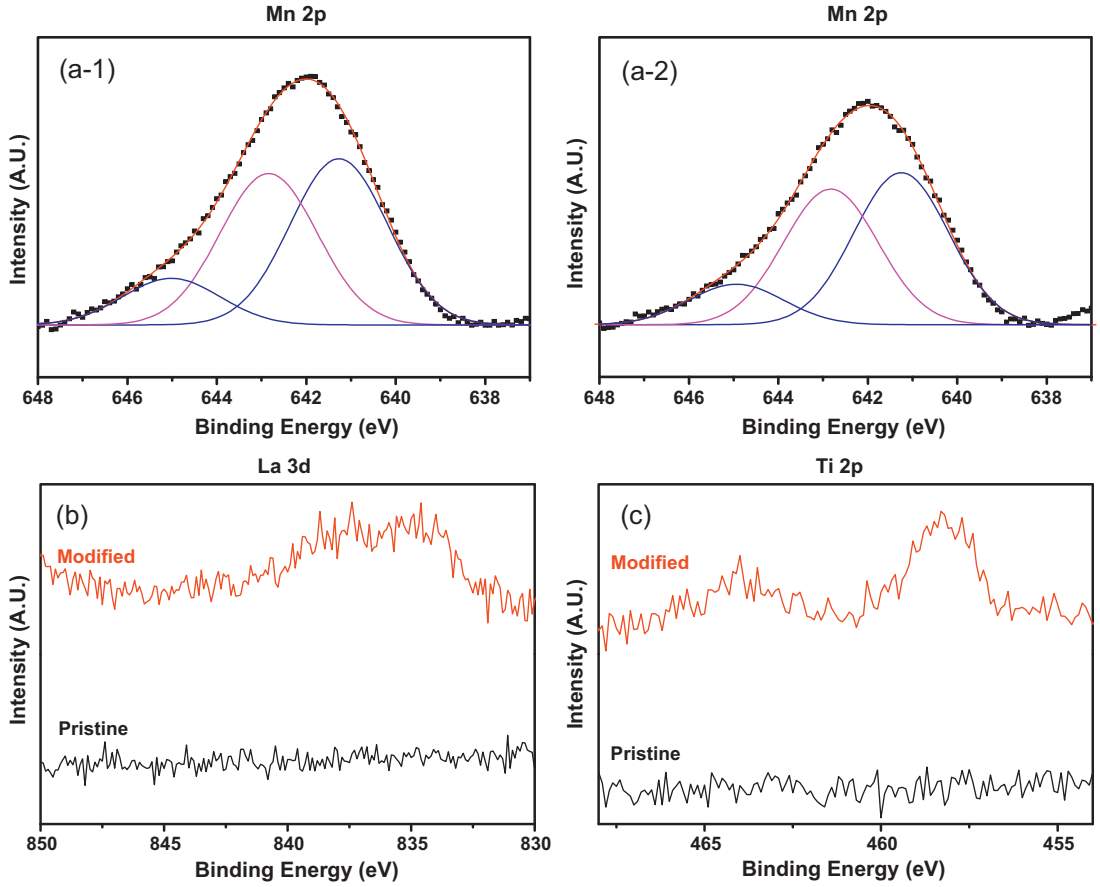

Fig. 2. XPS spectra of the pristine and [Li,La]TiO_3-modified $LiMn_2O_4$: (a) Mn, (b) La, (c) Ti (calculated Mn peaks (solid lines) with experimental data (square symbol) for the (a-1) pristine sample, (a-2) [Li,La]TiO_3-modified sample.

3. Results and discussion

The surface morphologies of the pristine and modified $LiMn_2O_4$ powders were observed by TEM analysis. As shown in Fig. 1(a), the pristine powder had a smooth, clean surface without any attached particles, whereas the crystal faces and edges of the modified powder were covered very homogeneously with a coating layer. In the TEM-EDS analysis, the main elements of the coating layer were confirmed as La, Ti, and O (and a small amount of Mn), which indicated that the coating layer formed successfully on the surface of the parent $LiMn_2O_4$ powder. The surface composition was also characterized by XPS. Fig. 2 shows the XPS data for the samples before and after the surface modification. The fitting results were compared to the experimental spectra in Fig. 2(a). The relative ratio of the area of Mn^{3+} and Mn^{4+} was calculated to determine the average oxidation state of the manganese. From the relative concentrations of Mn^{3+} and Mn^{4+}, the average oxidation state of the manganese corresponded to 3.54 for the pristine particles and 3.53 for the [Li,La]TiO_3-modified particles [33,34]. Note that the pristine sample had no La or Ti peaks that could be attributed to the surface-modified layers, whereas the modified material appeared to have La and Ti peaks, as shown in Fig. 2(b) and (c). Thus, La and Ti elements exist on the surface of the cathode material as a surface-modifying material, which is supported by the TEM-EDS analyses, as shown in Fig. 1. The XRD patterns of the pristine and [Li,La]TiO_3-modified $LiMn_2O_4$ powder were obtained to investigate the structural change after the coating process (not shown in the figures). Although a coating layer existed on the surface, the diffraction patterns of the coated powders were identical to those of the pristine sample. This suggests that the coating layer is an amorphous phase, as a heating temperature of 400 °C is not high enough to form a crystalline coating phase. In addition, it is likely that the coating process has no effect on the crystalline phase of the pristine powder.

The surface modification effect on the electrochemical properties of the pristine and modified electrode was characterized. Fig. 3 compares the discharge capacity of the pristine and [Li,La]TiO_3-modified $LiMn_2O_4$ electrodes at various current densities at an

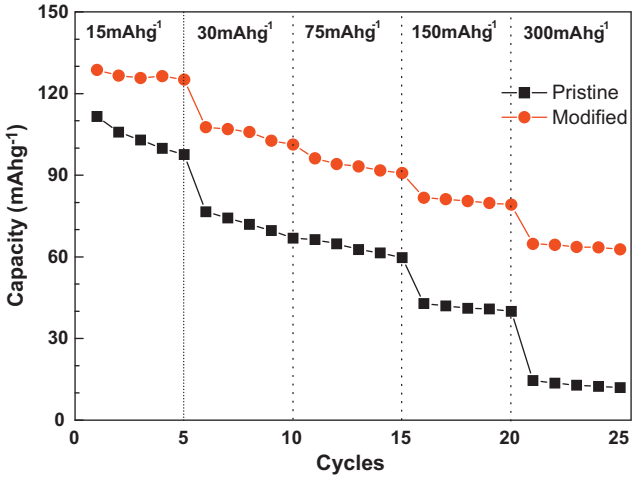

Fig. 3. Cycle performances of $LiMn_2O_4$ before and after surface modification at various current densities at 15 mA g^{-1}, 30 mA g^{-1}, 75 mA g^{-1}, 150 mA g^{-1} and 300 mA g^{-1} between 3.0 and 4.3 V (cells were tested at 65 °C).

Table 1
Specific initial discharge capacity and capacity retention data of $LiMn_2O_4$ before and after surface modification at various current densities (values of the first cycle). Percentages refer to the capacity retention compared with the discharge capacity at 15 mA g^{-1} (cells were tested at 65 °C).

Sample	Current density									
	15 mA g^{-1}		30 mA g^{-1}		75 mA g^{-1}		150 mA g^{-1}		300 mA g^{-1}	
	Initial capacity (mAh g^{-1})	Capacity retention (%)	Initial capacity (mAh g^{-1})	Capacity retention (%)	Initial capacity (mAh g^{-1})	Capacity retention (%)	Initial capacity (mAh g^{-1})	Capacity retention (%)	Initial capacity (mAh g^{-1})	Capacity retention (%)
Pristine	111.6	100	69	81	59	69	42.6	38	14.6	13
Modified	128.7	100	107.7	84	96.2	75	81.7	63	64.8	50

elevated temperature, where the samples were cycled 5 times at each current density. As shown in Fig. 3, the discharge capacity decreases as the current density increases in both powders, but the discharge capacity of the modified powder decreases more slightly than that of the pristine powder. The surface-modified electrode exhibits an improved discharge capacity relative to that of the pristine electrode throughout the current density range. Moreover, it is clear that the surface-modified electrodes have remarkably superior discharge capacities compared to the capacity of the pristine electrode as the current density increases. Capacity retention at 300 mA g^{-1} compared with that at 15 mA g^{-1} was only 13% for the pristine electrode. However, the surfaced-modified sample exhibited 50% capacity retention at the same current densities. The specific capacity and capacity retention data of the pristine and modified electrodes are given in detail in Table 1. This result confirms that the [Li,La]TiO_3 coating effectively enhances the rate capability. A stable coating layer protects the surfaces of the cathode and prevents the formation of unwanted interface layers that may originate from a reaction with the electrolyte; these protective and preventive behaviors enhance the rate capability. Moreover, the [Li,La]TiO_3 coating layer can act as a highly effective lithium ion conductor.

For a thorough investigation of the protective effect of the [Li,La]TiO_3 coating layer, the pristine and [Li,La]TiO_3-modified $LiMn_2O_4$ electrodes were stored at 65 °C and analyzed by XRD. As shown in Fig. 4, the pristine and modified samples, which were both stored for 50 h, exhibit similar patterns as the spinel phase without any second phase. However, after storage for 100 h, the XRD pattern of the pristine electrode appears to have second phase peaks. These peaks showed an increase after storage for 200 h. In contrast, the structural change of the modified $LiMn_2O_4$ electrodes was negligible after 100 h of storage. Although a phase change occurs in the modified $LiMn_2O_4$ electrodes after 200 h of storage, the intensity of the second phase peaks is considerably weaker than that of a pristine electrode. The second phase peak at a lower angle is indexed as MnO_2 (though a second phase peak is not identified at a higher angle). These results indicate that the [Li,La]TiO_3 coating suppresses the phase transition and increases the crystal stability of $LiMn_2O_4$ during storage, possibly due to the protection of the Mn dissolution. This will be correlated with the electrochemical properties of the electrodes.

Fig. 5 shows the microstructure of the pristine and modified $LiMn_2O_4$ electrodes stored at 65 °C for 200 h. Compared to the pristine electrode before storage in Fig. 1, the pristine electrode after storage shown in Fig. 5(a) exhibits an apparent change with respect to the shape of the particles. The shape of the particles in the pristine sample changed to a sphere shape without an edge. On the other hand, the modified $LiMn_2O_4$ in Fig. 5(b) shows a morphology that is similar to the initial modified $LiMn_2O_4$ before storage in Fig. 1. It is known that the change in the morphology with respect to dissolution starts at the edge part due to the higher surface energy there compared to that in other parts. Moreover, the amount of Mn dissolution for the pristine and modified $LiMn_2O_4$ powders was 0.147 ppm and 0.054 ppm, respectively. Thus, these results clearly indicate that the surface-modifying layer has the protective effect of Mn dissolution during storage in an electrolyte solution.

To obtain more information about the Mn dissolution during storage, the electrodes were investigated by GD-OES. In this method, the sputter progresses deeper into the electrode with time, and a depth profile of the constituent elements of the sample can be obtained. Fig. 6(a) shows the optical emissions from the constituent elements with the sputtering time for the pristine electrode before storage. Strong emission was observed from Mn, which is the main metal element in the electrode. In contrast, the emissions of La and Ti were not detected. The deviation of the emission intensity at the surface may be due to the roughness of the electrode. Compared to the profiles shown in Fig. 6(a) and (b) reveals that the GD-OES profiles of the pristine electrode were dramatically changed after storage at an elevated temperature. The emission intensity of Mn weakens from the surface to the current collector, and this changed profile was severe at the surface. This result clearly reveals that the Mn dissolved into the electrolyte from the surface of the electrode during storage. Fig. 7(a) shows the GD-OES profiles of the surface-modified $LiMn_2O_4$ cathodes before storage. The emission of the Ti element was clearly detected, and the optical emission

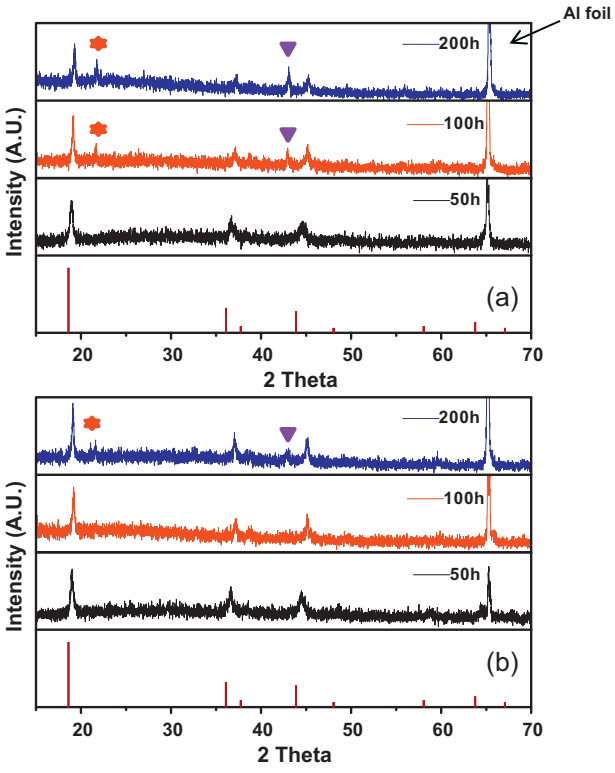

Fig. 4. Storage characteristics of the pristine and [Li,La]TiO_3-modified $LiMn_2O_4$: XRD patterns of the (a) pristine, (b) modified $LiMn_2O_4$.

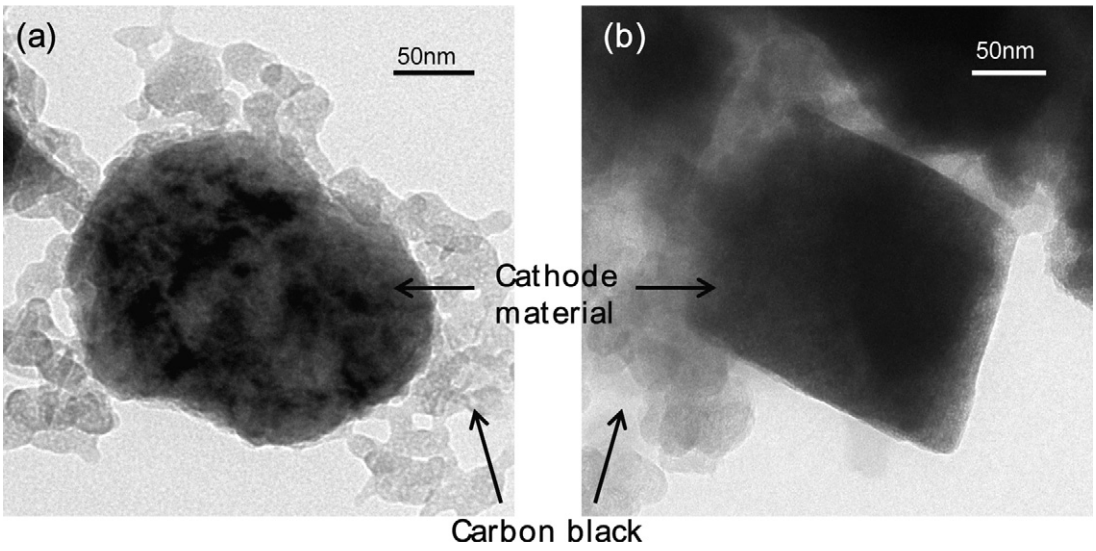

Fig. 5. Storage characteristics of the pristine and [Li,La]TiO_3-modified $LiMn_2O_4$: TEM images of the (a) pristine, (b) modified $LiMn_2O_4$ after storage.

profiles of the Mn element were similar to those of the pristine electrode. As shown Fig. 7(b), the GD-OES profile of the modified electrode also changed after storage. However, it is clear that the change of the profile of the optical emission of Mn during storage is severe according to the experimental results of the pristine electrode compared with the surface-modified $LiMn_2O_4$ electrode. This indicates that Mn dissolution into the electrolyte was suppressed by the [Li,La]TiO_3 coating layer.

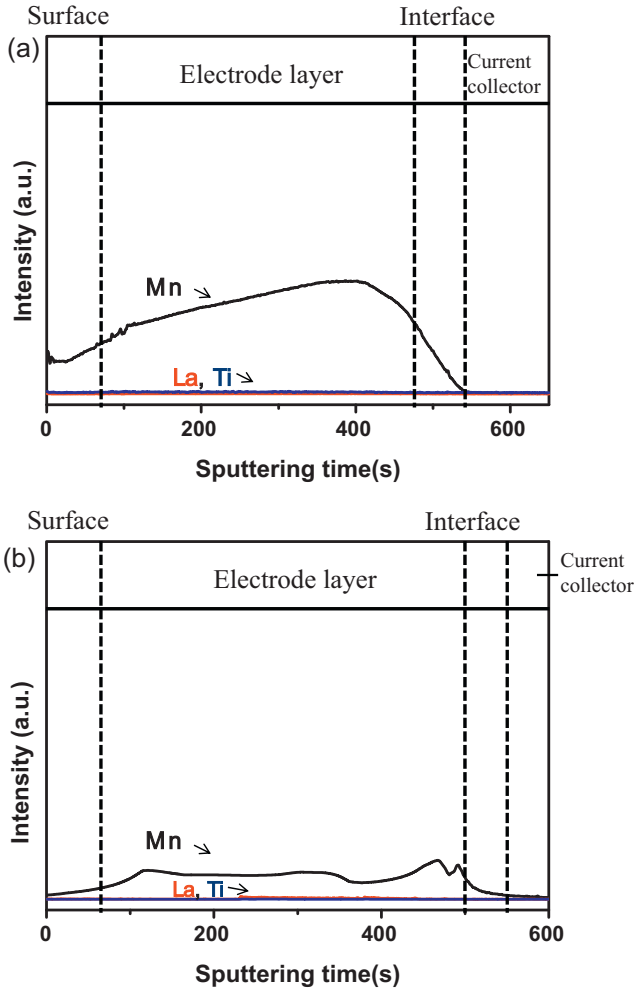

Fig. 6. Depth profiles of optical emission from constituent elements depending on sputtering time in GD-OES measurements of the pristine $LiMn_2O_4$ electrode: (a) before storage, (b) after storage at 60 °C for 200 h.

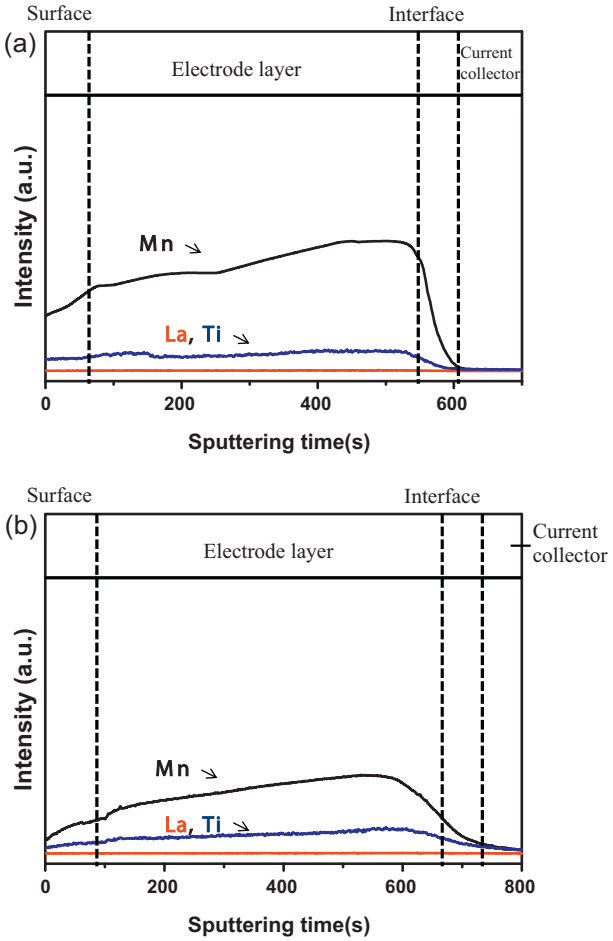

Fig. 7. Depth profiles of optical emission from constituent elements depending on sputtering time in GD-OES measurements of the [Li,La]TiO_3-modified $LiMn_2O_4$ electrode: (a) before storage, (b) after storage at 60 °C for 200 h.

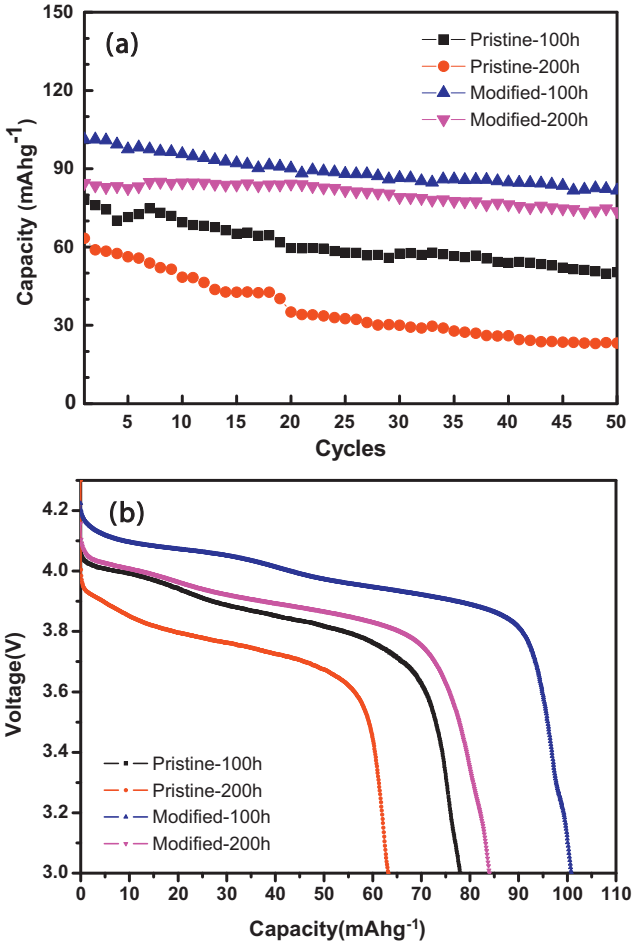

Fig. 8. Storage characteristics of the pristine and [Li,La]TiO_3-modified $LiMn_2O_4$: (a) initial capacity, (b) cycle performances at 30 mA g^{-1} of the pristine and modified $LiMn_2O_4$ electrodes stored at 65 °C between 3.0 and 4.3 V (cells were tested at room temperature).

The discharge capacity and cyclic performances after storage are shown in Fig. 8. The capacity loss during storage is much less in the surface-modified $LiMn_2O_4$ cathodes than in the pristine $LiMn_2O_4$ cathodes. The surface-modified $LiMn_2O_4$ cathode stored for 100 h provides a high initial capacity (101.3 mAh g^{-1}) and good cycle retention (81%). Though these values of the initial capacity and cycle retention decreased slightly after the storage process, the pristine cathode, even the sample stored for 100 h, showed a lower initial capacity and lower cycle retention compared to that of the surface-modified $LiMn_2O_4$ cathode stored for 200 h, also exhibiting a greatly inferior discharge property compared to the pristine cathode before storage. This result confirms that the highly protective effect of the [Li,La]TiO_3 coating discussed above enhances the electrochemical properties in terms of the initial capacity and capacity retention. Table 2 summarizes the specific initial discharge capacity and capacity retention data of $LiMn_2O_4$ after storage at 30 mA g^{-1}.

Table 2
Specific initial discharge capacity and capacity retention data of $LiMn_2O_4$ after storage at 30 mA g^{-1}. Percentages refer to the capacity retention during 50 cycles.

Sample	Storage time			
	100 h		200 h	
	Initial capacity (mAh g^{-1})	Capacity retention (%)	Initial capacity (mAh g^{-1})	Capacity retention (%)
Pristine	78.2	64	63.4	37
Modified	101.3	81	84.5	87

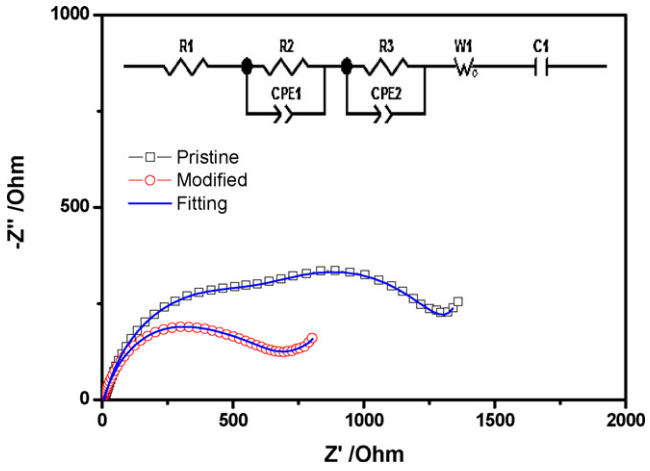

Fig. 9. Nyquist plots of the (a) pristine and (b) [Li,La]TiO_3-modified $LiMn_2O_4$ electrodes stored at 60 °C for 200 h after 50 cycles.

To obtain more information about the electrodes before and after storage, an impedance analysis was conducted. In general, the impedance spectra for a lithium battery test cell containing a cathode material exhibit two semicircles and a line inclined at a constant angle to the real axis. A high-frequency semicircle is involved in a passivating layer in what is known as the solid electrolyte interface, and the intermediate-frequency semicircle is related to the charge-transfer resistance in the electrode/electrolyte interface [35,36]. Fig. 9 shows the impedance spectra of the pristine and surface modified electrodes after 50 cycles. These electrodes were stored at 60 °C for 200 h before cycling. The inset of Fig. 9 presents the equivalent circuit used to fit the measured plots [37]. As shown in Fig. 9, the semicircles of the pristine electrode were two times larger than those of the modified electrode. The fitted values of both the high-frequency and intermediate-frequency semicircles of the modified electrode were only 323 Ω and 301 Ω, respectively. However, those of the pristine electrode were 567 Ω and 774 Ω, respectively. Thus, it is clear that impedance growth at a solid electrolyte interface and charge-transfer resistance are effectively suppressed by a [Li,La]TiO_3 coating layer during cycling. The data in the XRD patterns in Fig. 4, TEM images in Fig. 5, GD-OES profiles in Figs. 6 and 7 and the EIS plots shown in Fig. 9 all indicate that a [Li,La]TiO_3 coating layer prevents the growth of interfacial resistance through the suppression of the Mn dissolution and the unwanted side reactions related to the Mn dissolution. This is associated with enhanced electrochemical properties, as shown in Fig. 8.

4. Conclusions

A novel coating material [Li,La]TiO_3 was introduced for the $LiMn_2O_4$ cathode, and the surface modification effects were examined. The discharge capacity and rate capability were both enhanced by the successfully coated [Li,La]TiO_3 layer on $LiMn_2O_4$. In the storage test at 65 °C, the modified $LiMn_2O_4$ electrode showed a more stable structure and surface morphology against contact with electrolytes than the pristine electrode. In addition, Mn dissolution was also significantly decreased by [Li,La]TiO_3 coating. These results correlated with an enhanced electrochemical property and a decreased interfacial resistance of the modified electrode after storage, compared with those of the pristine electrode. This study confirmed that [Li,La]TiO_3 coating is very effective as surface protection from the unwanted reaction between the a cathode and an electrolyte.

Acknowledgement

This research was supported by the Converging Research Center Program through the Ministry of Education, Science and Technology (2010K001089).

References

[1] E. Hosono, T. Kudo, I. Honma, H. Matsuda, H. Zhou, Nano Lett. 9 (2009) 1045.
[2] T.F. Yi, Y.R. Zhu, X.D. Zhu, J. Shu, C.B. Yue, A.N. Zhou, Ionics 15 (2010) 779.
[3] Y. Zhang, L.Z. Ouyang, C.Y. Chung, M. Zhu, J. Alloys Compd. 480 (2010) 981.
[4] S.N. Karthick, S.R.P. Gnanakan, A. Subramania, H.J. Kim, J. Alloys Compd. 489 (2010) 674.
[5] P. Piszora, J. Alloys Compd. 401 (2005) 34.
[6] Q. Liu, L. Yu, H. Wang, J. Alloys Compd. 486 (2009) 886.
[7] S. Hirose, T. Kodera, T. Ogihara, J. Alloys Compd. 506 (2010) 883.
[8] M.M. Thackeray, C.S. Johnson, J.S. Kim, K.C. Lauzze, J.T. Vaughey, N. Dietz, D. Abraham, S.A. Hackney, W. Zeltner, M.A. Anderson, Electrochem. Commun. 5 (2003) 752.
[9] J. Tu, X.B. Zhao, J. Xie, G.S. Cao, D.G. Zhuang, T.J. Zhu, J.P. Tu, J. Alloys Compd. 432 (2007) 313.
[10] D. Arumugam, G.P. Kalaignan, Electochim. Acta 55 (2010) 8709.
[11] X. Li, Y. Xu, C. Wang, J. Alloys Compd. 479 (2009) 310.
[12] M. Nakayama, M. Nogami, Solid State Commun. 150 (2010) 1329.
[13] S. Komaba, A. Ogata, T. Shimizu, S. Ikemoto, Solid State Ionics 179 (2008) 1783.
[14] L. Zhang, X. Lv, Y. Wen, F. Wang, H. Su, J. Alloys Compd. 480 (2009) 802.
[15] G.Q. Liu, L. Wen, G.Y. Liu, Y.W. Tian, J. Alloys Compd. 501 (2010) 233.
[16] T. Yang, K. Sun, Z. Lei, N. Zhang, Y. Lang, J. Alloys Compd. 502 (2010) 215.
[17] K.N. Jung, S.I. Pyun, Electrochim. Acta 52 (2007) 5453.
[18] J.S. Gnanaraj, V.G. Pol, A. Gedanken, D. Aurbach, Electrochem. Commun. 5 (2003) 940.
[19] A.M. Kannan, A. Manthiram, Electrochem. Solid-State Lett. 5 (2002) A167.
[20] J.W. Lee, S.M. Park, H.J. Kim, Electrochem. Commun. 11 (2009) 1101.
[21] Y. Inaguma, Y. Matsui, Y.J. Shan, M. Itoh, T. Nakamura, Solid State Ionics 79 (1995) 91.
[22] M. Oguni, Y. Inaguma, M. Itoh, T. Nakamura, Solid State Commun. 91 (1994) 627.
[23] M.H. Bhat, A. Miura, P. Vinatier, A. Levasseur, K.J. Rao, Solid State Commun. 125 (2003) 557.
[24] Y. Inaguma, C. Liquan, M. Itoh, T. Nakamura, T. Uchidam, H. Ikuta, M. Wakihara, Solid State Commun. 86 (1993) 689.
[25] L.X. He, H.I. Yoo, Electrochim. Acta 48 (2003) 1357.
[26] Y. Maruyama, H. Ogawa, M. Kamimura, S. Ono, Ionics 14 (2008) 357.
[27] N. Inoue, Y. Zou, Solid State Ionics 176 (2005) 2341.
[28] S.T. Myung, K. Izumi, S. Komaba, H. Yashiro, H.J. Bang, Y.K. Sun, N. Kumagai, J. Phys. Chem. C 111 (2007) 4061.
[29] H.J. Lee, K.S. Park, Y.J. Park, J. Power Sources 195 (2010) 6122.
[30] K.S. Ryu, S.H. Lee, B.K. Koo, J.W. Lee, K.M. Kim, Y.J. Park, J. Appl. Electrochem. 38 (2008) 1385.
[31] Q.T. Qu, G.J. Wang, L.L. Liu, S. Tian, Y. Shi, Y.P. Wu, Funct. Mater. Lett. 3 (2010) 151.
[32] W. Tang, S. Tian, L.L. Liu, L. Li, H.P. Zhang, Y.B. Yue, Y. Bai, Y.P. Wu, K. Zhu, Electrochem. Commun. in press.
[33] N. Treuil, C. Labrugere, M. Menetrier, J. Portier, J. Portier, G. Campet, A. Deshayes, J.C. Frison, S.J. Hwang, S.W. Song, J.H. Choy, J. Phys. Chem. B 103 (1999) 2100.
[34] Y. Liu, X. Li, H. Guo, Z. Wang, Q. Hu, W. Peng, Y. Yang, J. Power Sources 189 (2009) 721.
[35] T.L Kulova, V.A. Tarnopol, A.M. Skundin, Russ. J. Electrochem. 45 (2009) 38.
[36] A.K. Hjelm, G. Lindbergh, Electrochim. Acta 47 (2002) 1747.
[37] J.M. Zheng, Z.R. Zhang, X.B. Wu, Z.X. Dong, Z. Zhu, Y. Yang, J. Electrochem. Soc. 155 (2008) A775.